Drag on Spheroidal Particles in Dilatant Fluids

A. Tripathi and R. P. Chhabra
Dept. of Chemical Engineering, Indian Institute of Technology, Kanpur, India 208016

In recent years, considerable interest has been shown in studying the motion of spherical and nonspherical particles in a variety of non-Newtonian fluids. It is readily recognized that the parameter of central interest here is the drag force experienced by a solid particle moving through a liquid medium. This information is conveniently expressed via the use of dimensionless groups such as drag coefficient, Reynolds number and non-Newtonian parameters; the exact number and form of the latter depend upon the choice of a specific rheological model. Admittedly a wealth of information is now available on the motion of spherical and nonspherical particles in non-Newtonian media; however, a cursory inspection of the most recent survey clearly shows that most of it relates to the drag on spherical particles in pseudoplastic, viscoplastic and viscoelastic fluids (Chhabra, 1993). In contrast, very little information is available on the analogous situation involving spherical and nonspherical solid particles moving in shear thickening fluids. Indeed, to the best of our knowledge, there have been only three studies on the motion of spheres in dilatant fluids. Tomita (1959) employed an approximate velocity variational principle to estimate the drag on a sphere moving slowly (zero Reynolds number) through power law type dilatant fluids. His results have been corrected subsequently by Wallick et al. (1962). More recently, Jaiswal (1991) presented limited numerical results for drag on spheres in dilatant fluids in the creeping regime ($Re = 0.001$). Prakash (1976) reported a few experimental values of drag coefficient for spheres settling through a starch solution ($n = 1.2$); however, all his data points relate to the particle Reynolds number greater than 1,000 and hence a direct comparison with the aforementioned theoretical analyses is not possible.

One may conclude that very little information is available on the drag of spherical particles in dilatant fluids, while no results have been reported to date for prolate and oblate shaped objects. In this work extensive theoretical results on drag coefficients for spheres, prolates, and oblates as functions of aspect ratio (E), particle Reynolds number (Re), and the flow behavior index (n) are presented and discussed in the following ranges of conditions:

$$1 \le n \le 1.8;\ 0.2 \le E \le 5 \text{ and } 0.001 \le Re \le 100$$

Correspondence concerning this article should be addressed to R. P. Chhabra at: School of Chemical Engineering and Industrial Chemistry, University of New South Wales, Sydney NSW, Australia 2052.
Current address of A. Tripathi: Dept. of Chemical Engineering, The Levich Institute, CUNY, New York, NY 10031.

Problem Statement and Numerical Formulation

Consider the steady and incompressible flow of a power law type dilatant fluid ($n > 1$) past an axisymmetric solid particle, as shown in Figure 1. The equations of continuity and momentum, in their vectorial and nondimensional form, respectively are written as:

$$\nabla^* \cdot \mathbf{v}^* = 0 \tag{1a}$$

$$\mathbf{v}^* \cdot \nabla^* \mathbf{v}^* = -\nabla^* p^* + (2^n/Re)\{\nabla^* \cdot [\eta^*(\nabla^* \mathbf{v}^* + (\nabla^* \mathbf{v}^*)^T)]\} \tag{1b}$$

where the gravity has been absorbed into the pressure term. The rheological behavior of a power law model fluid is expressed as:

$$\eta^* = (\Pi^*/2)^{(n-1)/2} \tag{2}$$

The pertinent boundary conditions for this flow configuration are those of the free stream velocity far away from the particle and that of no slip on the particle surface, that is:

$$\text{At } r^* = R^*(\theta) \quad v_x^* = v_y^* = 0 \tag{3a}$$

$$\text{At } r^* \to \infty \quad v_x^* = 1;\ v_y^* = 0 \tag{3b}$$

where subscripts x and y denote the axial and radial directions respectively (see Figure 1). Furthermore, the axisymmetry condition is applied by prescribing $\partial v_x^*/\partial y^* = 0$ and $v_y^* = 0$ on the x axis.

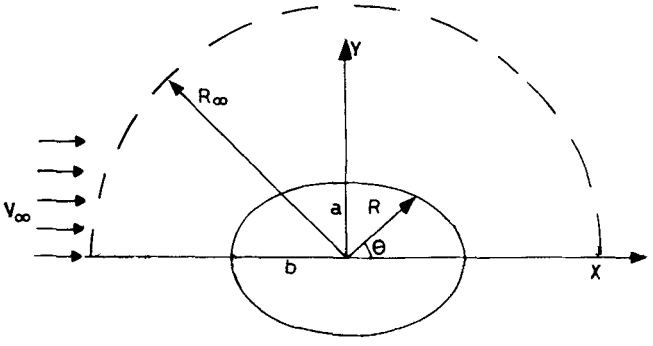

Figure 1. Flow representation.

The aforementioned equations and conditions have been normalized as follows:

$$\mathbf{v}^* = \mathbf{v}/v_\infty;\ \nabla^* = R_{eq}\nabla;\ \eta^* = \eta/\eta_{ref};\ x^* = x/R_{eq}$$

$$y^* = y/R_{eq};\ \eta_{ref} = K(v_\infty/R_{eq})^{n-1};\ p^* = p/\rho v_\infty^2$$

$$\tau_{ij}^* = \tau_{ij}/(\eta_{ref} v_\infty/R_{eq});\ \Pi^* = \Pi(R_{eq}/v_\infty)^2;$$

$$Re = \rho(2R_{eq})^n v_\infty^{2-n}/K \quad (4)$$

In Eq. 4, R_{eq}, the equivalent volume sphere radius, is defined as:

$$R_{eq} = \left(\frac{3v}{4\pi}\right)^{1/3} = \left[\frac{1}{2}\int_0^\pi \{R(\theta)\}^3 \sin\theta\, d\theta\right]^{1/3} \quad (5)$$

where $R(\theta)$, the surface of the particle, is conveniently expressed as:

$$R(\theta) = \frac{ab}{(a^2\cos^2\theta + b^2\sin^2\theta)^{1/2}} \quad (6)$$

Thus, for a specified volume of particle, it is sufficient to select only a or b to generate different shapes, but it is customary to use an aspect ratio, $E = b/a$, as a prescribed parameter to denote oblate ($E<1$) and prolate ($E>1$) shapes. A reference frame attached to the centroid of the particle is chosen for convenience.

Equations 1 to 6 are the final working equations describing the flow of a power law fluid past an axisymmetric particle, which have been solved numerically using the finite-element method. Since the detailed descriptions of the numerical solution procedure, as well as the methodology for post processing the detailed velocity and pressure fields to obtain the values of drag coefficients (pressure and friction), are available elsewhere; these are not repeated here (Jaiswal et al., 1992; Tripathi et al., 1994).

Results and Discussion

In this work, the friction, pressure and total drag coefficients have been calculated in the following ranges of conditions, $1 \le n \le 1.8$; $0.2 \le E \le 5$ and $0.001 \le Re \le 100$. In addition, limited results for streamline patterns showing the onset of wake formation and so on are also computed. Prior to the presentation of new results, the present results have been compared with the previous analytical/numerical and experimental results for several limiting cases.

Results Validation

The present results for $E=1$ and $n=1$, that is, spheres in Newtonian fluids are in excellent agreement with the previous numerical (LeClair, 1970) and the "best" experimental results (Clift et al., 1978); the maximum discrepancy being of the order of 0.6% from numerical results and about 6% from experiments in the range $0.001 \le Re \le 100$. Likewise, the computed and prior analytical/numerical velocity and pressure profiles are also in complete agreement in the whole range of Reynolds numbers considered herein. Analogous comparisons for spheroidal particles moving in Newtonian fluids with the analytical and numerical results of Masliyah and Epstein (1970) revealed an excellent match in the creeping flow region ($\pm 0.3\%$), with a slight deterioration in correspondence at high Reynolds numbers; the maximum discrepancy being 10% at $Re = 100$. Present predictions are also consistent ($\pm 9\%$) with a recently proposed correlation for drag of oblates and prolates (Militzer et al., 1989). Finally, the present values of C_D for spheres at low Reynolds numbers ($Re = 0.001$) are contrasted with the corresponding results reported by Tomita (1959), (as corrected by Wallick et al., 1962) and by Jaiswal (1991) in Figure 2. While an excellent match is seen to exist between the present results and those of Jaiswal (1991), significant deviations occur from the approximate results of Tomita (1959). Though possible reasons for the latter discrepancy are not immediately obvious, at least part of it must be due to the inadequacy of the trial flow field assumed by Tomita (1959), which only satisfied the equation of continuity and the boundary conditions and not the momentum equation. Finally, as expected, the dependence of the drag correction factor on the flow behavior index is seen to be opposite of that for shear thinning power law fluids (Chhabra, 1993). Based on these comparisons, it is perhaps reasonable to state that the values of drag coefficient for spheroids in power law fluid are reliable to within $\pm 1\%$.

Drag Phenomena for Spheroids

Table 1 summarizes the computed values of drag coefficient for a range of values of the particle Reynolds number (0.001 to 100), the flow behavior index (1 to 1.8), and the aspect ratio (0.2 to 5). Qualitatively, the dependence of the drag coefficient on the flow behavior index is seen to be similar for both

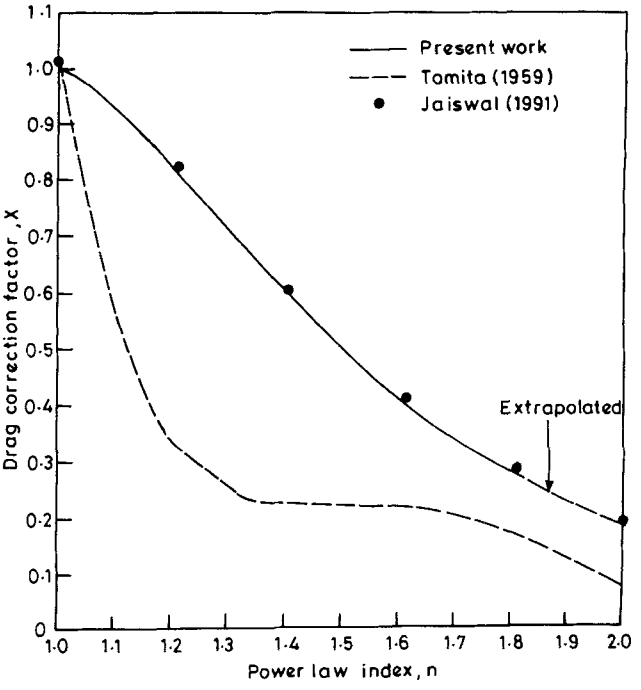

Figure 2. Present vs. previous results for spheres in shear thickening fluids in low Reynolds number region.

spherical as well as spheroidal particles. Also, the flow behavior index is seen to exert more influence on drag in the low Reynolds number region (up to about $Re \simeq 1$), whereas the Reynolds number seems to be a more significant variable than the flow behavior index in the $Re > 1$ region. For instance, for $Re = 0.01$, the drag coefficient decreases almost by a factor of 3 as the flow behavior index rises from 1 to 1.8. The corresponding change is only of the order of 30–40% at $Re = 100$, however. This suggests that for $Re > 10$ or so, the viscous effects gradually diminish and the value of drag is governed largely by the inertial forces. Likewise, for fixed values of n and Re, the value of the drag coefficient deviates increasingly with the increasing nonsphericity; however, the effect appears to be more striking in the low Re region. Further examination of Table 1 shows that at low Re, an oblate spheroid ($E < 1$) with large aspect ratio results in lower drag than a sphere, but eventually this tendency is reversed at high Reynolds number; this switch-over behavior is related to the fact that at high Re, the wake grows in size thereby leading to a larger value of C_D.

Some further insight into the drag phenomena can be gained by examining the variation of the pressure to friction drag ratio with the system variables. Figure 3 displays the dependence of (C_{DP}/C_{DF}) as a function of the aspect ratio and the particle Reynolds number, for two values of $n = 1$, and $n = 1.8$. Again, the dependence is seen to be qualitatively similar for Newtonian and shear thickening fluids. However, the pressure drag contribution rises with the increasing particle Reynolds number; though the shear thickening behavior seems to suppress the increase. For instance, for $n = 1$, C_{DP}/C_{DF} is seen to range from 2.2 to ~ 7 as the Reynolds number varies from 0.01 to 100 for an oblate with $E = 0.2$; the corresponding variation is only from about 0.9 to 1.55 for $n = 1.8$. Furthermore, for prolates ($E > 1$), the drag ratio (C_{DP}/C_{DF}) is virtually unaffected by the value of Reynolds number but monotonically decreases with the increasing value of n. After the initial decrease as n increases from 1 to 1.2, the value of (C_{DP}/C_{DF}) is almost independent of the subsequent variation in the value of n.

For a few cases, the streamline patterns were also analyzed in detail, with a view to delineate the role of shear thickening behavior on the flow field, wake formation, the size of the wake, and so on. The main findings can be summarized as follows: for a sphere, the flow field exhibits fore-and-aft symmetry up to about $Re \simeq 10$. A clear wake develops at $Re \sim 20$. This behavior was observed for all values of n $(1 \leq n \leq 1.8)$. This suggests that the detailed flow field is somewhat insensitive to the type of fluid as well as the extent of non-Newtonian behavior, though the drag is strongly dependent on the value of n, as seen above. Indeed, even for spheroidal particles, the flow structures for Newtonian and shear thickening materials were virtually indistinguishable from each other. For example,

Table 1. Computed Values of Drag Coefficient

Re / n	0.001	0.01	1	10	50	100
			$E = 5.0$			
1	43,823.63	4,382.37	48.569	6.939	2.097	1.264
1.2	34,158.053	3,415.806	43.184	6.8995	2.0227	1.223
1.4	24,777.081	2,477.713	38.589	6.774	2.008	1.171
1.6	16,978.391	1,697.84	34.547	6.3926	1.983	1.073
1.8	11,358.077	1,135.808	31.129	6.078	1.813	1.042
			$E = 2.0$			
1	29,506.81	2,950.69	32.687	4.768	1.605	1.119
1.2	23,073.68	2,307.37	29.232	4.698	1.594	1.046
1.4	16,827.23	1,682.73	25.719	4.597	1.567	1.019
1.6	11,604.18	1,160.42	23.256	4.350	1.418	0.932
1.8	7,826.51	782.657	20.608	4.25	1.396	0.823
			$E = 1$			
1	24,001.03	2,400.190	27.150	4.2604	1.57	1.083
1.2	19,845.41	1,984.55	24.157	4.208	1.552	1.030
1.4	13,665.79	1,366.583	21.270	4.108	1.519	0.977
1.6	9,367.53	936.762	19.4344	4.0772	1.4486	0.886
1.8	6,275.687	627.57	17.078	3.71	1.2918	0.784
			$E = 0.50$			
1	22,313.08	2,231.31	25.176	4.3318	1.7328	1.1744
1.2	16,818.89	1,681.898	21.909	4.3065	1.7239	1.1322
1.4	11,908.51	1,190.859	19.148	4.255	1.6334	1.0373
1.6	8,056.19	805.624	17.019	4.015	1.4797	0.9186
1.8	5,337.78	533.789	15.661	3.664	1.3114	0.7999
			$E = 0.2$			
1	21,260.37	2,126.04	24.68	4.666	2.199	1.607
1.2	15,384.63	1,538.50	20.976	4.635	2.042	1.3257
1.4	10,548.03	1,054.82	18.029	4.573	1.8596	1.168
1.6	6,950.49	695.06	16.047	4.228	1.643	1.0105
1.8	4,507.48	450.756	14.015	3.825	1.425	0.8715

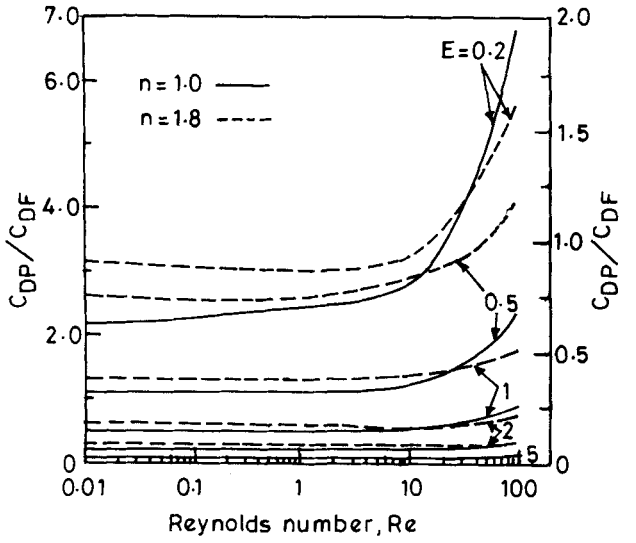

Figure 3. Dependence of (C_{DP}/C_{DF}) on Reynolds number and aspect ratio for $n=1$ (lefthand Y scale) and $n=1.8$ (righthand Y scale).

no visible wake appeared for prolates with $E=5$ even up to $Re=100$, whereas a wake forms for oblates at a lower Reynolds number than that in the case of a sphere.

As remarked earlier, the limited experimental results available on the drag of spheres (Prakash, 1976) in dilatant fluids relate to $Re>1{,}000$ and hence a direct comparison with the present results is not possible.

Conclusions

Theoretical estimates of drag coefficients for spheres, prolates and oblates moving in dilatant fluids have been obtained. The effect of the flow behavior index on drag coefficient in dilatant fluids is reverse of that observed in shear thinning fluids. Qualitatively, the dependence of drag on the flow behavior index is similar for both spherical and spheroidal particles. The total drag on oblates is lower than that for spheres in the viscous region, whereas it is the other way round at high Reynolds numbers and vice versa for prolates. The pressure drag contribution rises with the increasing particle Reynolds number. However, the extent of rise of this contribution diminishes with the increasing value of n. Furthermore, this phenomenon is much more striking for oblates than in the case of prolates; in the latter case, the pressure to friction drag ratio deviates little from its value in the creeping flow region. An examination of limited streamline patterns suggests that these are unaffected by the extent of non-Newtonian behavior. Unfortunately, no suitable experimental results are available in the literature to validate the theoretical predictions.

Notation

a, b = semiaxes of particle normal to and along the flow respectively, m
C_D = drag coefficient ($=C_{DP}+C_{DF}$)
C_{DF} = friction drag coefficient
C_{DP} = pressure drag coefficient
E = aspect ratio ($=b/a$)
F_D = drag force, $N(=C_D\cdot(1/2)\rho v_\infty^2\pi R_{eq}^2)$
K = power law consistency index, Pa·s^n
n = flow behavior index
p = pressure, Pa
r = radial coordinate, m
$R(\theta)$ = particle radius, m
R_{eq} = volume equivalent sphere radius, m
Re = Reynolds number
x, y = axial and radial coordinates, m
X = drag correction factor ($=C_DRe/24$)
v = volume of particle, m^3
$\mathbf{v}$ = velocity vector, m/s
v_∞ = free stream velocity, m/s
v_x, v_y = components of v, m/s

Greek letters

∇ = del operator, m^{-1}
η = apparent viscosity, Pa·s
θ = polar angle
Π = second invariant of rate of deformation tensor, s^{-2}
ρ = fluid density, Kg·m^{-3}

Subscripts

$*$ = dimensionless quantitiy

Literature Cited

Chhabra, R. P., "Bubbles, Drops and Particles in Non-Newtonian Fluids," CRC Press, Boca Raton, FL (1993).

Clift, R., J. Grace, and M. E. Weber, *Bubbles, Drops and Particles*, Academic, New York (1978).

Jaiswal, A. K., Unpublished Work, Indian Inst. of Technology, Kanpur, India (1991).

Jaiswal, A. K., T. Sundararajan, and R. P. Chhabra, "Simulation of Non-Newtonian Fluid Flow Through Fixed and Fluidized Beds of Spherical Particles," *Num. Heat Transf.*, **21A**, 275 (1992).

LeClair, B. P., PhD Thesis, McMaster Univ., Hamilton, Ont., Canada (1970).

Masliyah, J. H., and N. Epstein, "Numerical Study of Steady Flow Past Spheroids," *J. Fluid Mech.*, **44**, 493 (1970).

Militzer, J., J. M. Kan, F. Hamdullahpur, P. R. Amyotte, and A. M. Al Taweel, "Drag Coefficient for Axisymmetric Flow Around Individual Spheroidal Particles," *Powder Technol.*, **57**, 193 (1989).

Prakash, S., M.Tech Dissertation, Banaras Hindu University, Varanasi, India (1976).

Tomita, Y., "On the Fundamental Formula of Non-Newtonian Flow," *Bull. Jap. Soc. Mech. Engrs.*, **2**, 469 (1959).

Tripathi, A., R. P. Chhabra, and T. Sundararajan, "Power Law Fluid Flow over Spheroidal Particles," *Ind. Eng. Chem. Res.*, **33**, 403 (1994).

Wallick, G. C., J. G. Savins, and D. R. Arterburn, "Tomita Solution for the Motion of a Sphere in a Power Law Liquid," *Phys. Fluids*, **5**, 367 (1962).

Manuscript received Aug. 16, 1993, and revision received Mar. 11, 1994.